

The Role of r-Modes in Pulsar Spin-down, Pulsar Timing and Gravitational Waves

Varenja Upadhyaya,^{a,1} Xiyuan Li,^b Xiyang Zhangs^c Shahram Abbassi^b S. R. Valluri,^b

^aDepartment of Physics, Indian Institute of Technology, Hyderabad, Telangana-502284, India

^bDepartment of Physics and Astronomy, University of Western Ontario, London, ON, N6A 3K7, Canada

^cDepartment of Statistical and Actuarial Sciences, University of Western Ontario, London, ON, N6A 3K7, Canada

E-mail: ep20btech11026@iith.ac.in, xli2522@uwo.ca, xzha272@uwo.ca, sabbassi@uwo.ca, valluri@uwo.ca

Abstract. We investigate the role of r-modes in the spin-down of pulsars, focusing on their implications for pulsar timing and gravitational wave emissions. Our study employs a non-linear differential equation incorporating the contribution of r-modes to derive time-dependent rotational frequency and period functions. This model is validated against observational data from the Crab pulsar, demonstrating a high degree of accuracy. By fitting the braking indices and spin-down coefficients, we establish direct and analytical relationships between observable pulsar properties and weak gravitational wave signals. We also derive analytical expressions for neutron star compactness and tidal deformability using Lambert W solutions, independent of the equation of state (EoS). These solutions provide new insights into the mathematical relationships between physical quantities, constraining the parameter space for r-mode gravitational wave frequency searches. Our results show that incorporating r-modes significantly enhances our ability to measure the neutron star EoS and predict pulsar age, rotational velocity, and gravitational wave frequencies. The seventh-order approximation used in our model is essential for accurately capturing the contributions of r-modes to the spin-down process. This framework can be applied to model pulsar timing residuals, account for glitches, and improve the detection and analysis of continuous gravitational waves from pulsars. With the advent of next-generation gravitational wave detectors, our findings offer promising prospects for disentangling individual events from the stochastic gravitational wave background, advancing our understanding of neutron star interiors and their dynamic processes.

Keywords: Accretion – post-Newtonian – gravity – hydrodynamics

¹Corresponding author.

Contents

1	Introduction	1
2	Spindown Mechanisms	2
3	Analytical Expressions considering r-modes	4
3.1	Rotational Frequency and r-Mode Frequency	4
3.2	Compactness and r-Mode Frequency	5
3.3	Tidal Deformability and r-Mode Frequency	6
3.4	r-Mode Amplitude and Rotational Frequency	7
3.5	Period and Time-Dependent Spin-down Coefficients	8
3.6	Braking Indices	10
4	Period Analysis with Glitching Crab Pulsar PSR B0531+21 Data	12
5	Discussion	14
6	Conclusions	16
A	Frequency Cubic Roots with Time-independent Coefficients	17
B	Period Analysis with Cubic Roots	18

1 Introduction

R-modes, akin to Rossby waves in Earth's oceans, are inertial oscillations in rotating stars driven by the Coriolis force. These predominantly toroidal modes have oscillation frequencies proportional to the star's rotation rate [1, 2]. In pulsars, the r-mode instability is particularly noteworthy due to its potential as a gravitational wave source [3, 4, 5]. The instability arises when gravitational radiation emitted by the oscillating mode extracts more angular momentum than is internally dissipated, causing the mode's amplitude to grow exponentially and facilitating rapid angular momentum loss [6].

Pulsars, highly magnetized, fast-spinning neutron stars, emit beams of electromagnetic radiation from their poles, detectable when the beam shines on Earth. This "lighthouse effect" has led to them being referred to as "Cosmic Lighthouses" [7]. Neutron stars, remnants of stars after supernovae, retain most of their angular momentum and, despite significant loss of moment of inertia during the supernova, exhibit high rotational speeds that gradually decrease over time due to energy loss until they 'turn off' [8]. The terms pulsar and rotating neutron star are used interchangeably throughout this paper.

The dissipation of r-modes represents a significant potential source of continuous gravitational waves, detectable by observatories such as LIGO, Virgo, and KAGRA [9, 10]. Gravitational wave astronomy, though relatively new, has made substantial contributions to astrophysics since the first detection of a gravitational wave event, GW150914, in 2015, generated by a binary black hole merger [9]. Since then, LIGO and Virgo have confirmed nearly 100 detections [11], with KAGRA contributing during the O3b observing run [10].

The r-mode instability can significantly affect the rotational evolution of pulsars, potentially reducing their frequencies [12]. Extensive studies have explored factors such as magnetic fields, differential rotation, superfluidity, and crust elasticity on the growth and saturation of r-modes [13, 14, 15, 16]. Rapidly rotating pulsars are promising sources of continuous quasi-monochromatic gravitational waves [17]. Two important emission mechanisms are a non-axisymmetric mass quadrupole and a current-quadrupole r-mode [18]. Detecting these waves is challenging but crucial for studying the neutron star equation of state (EoS) [19]. The gravitational wave frequencies of several known pulsars fall within the most sensitive bands of LIGO, Virgo, and KAGRA detectors [20, 21, 22], making them prime targets for continuous wave searches [19]. The advent of third-generation detectors like the Einstein Telescope [23], Cosmic Explorer [24], and space-based detectors like LISA [25], Taiji [26], and Tianqin [27], will enhance prospects of detecting continuous gravitational waves from slowly rotating pulsars and binary neutron star coalescence.

The radio waves emitted by pulsars can be precisely timed, akin to clock ticks. Millisecond pulsars, which spin hundreds of times per second, exhibit remarkable stability comparable to atomic clocks on Earth [28, 29]. Pulsar Timing Arrays (PTA) leverage this stability to detect gravitational waves by analyzing correlated pulse arrival times across multiple pulsars. PTAs are sensitive probes for detecting gravitational waves propagating through spacetime [30, 31, 32]. Several consortia, including the European Pulsar Timing Array [33], Indian Pulsar Timing Array [34], Parkes Pulsar Timing Array [35], Chinese Pulsar Timing Array [36], NANOGrav [37], and the Square Kilometer Array [38], are actively utilizing PTAs for gravitational wave detection in nanohertz-microhertz frequencies.

This research aims to refine our understanding of r-mode instability conditions and assess the detectability of resulting gravitational waves. Validating r-mode instability through gravitational wave detection would confirm theoretical predictions and provide insights into pulsar physics and internal structure [39, 40]. Such findings would advance multi-messenger astronomy by linking gravitational wave signals with electromagnetic observations, enhancing our knowledge of the extreme conditions in pulsars and fundamental physics.

Following Chishtie et al. [41], this paper considers a time-dependent r-mode frequency and amplitude model accounting for electromagnetic, gravitational wave, and r-mode energy losses. We provide a direct Lambert-Tsallis solution for pulsar rotational frequency in terms of r-mode gravitational wave frequency. We modify common quadratic fitting functions, presenting direct expressions for pulsar compactness and tidal deformability using the Lambert-W function.

Section 2 discusses pulsar spin-down and energy loss mechanisms. Section 3 presents pulsar rotational frequency, compactness, tidal deformability, r-mode amplitude, and pulsar period in terms of r-mode gravitational wave frequency. Section 4 compares numerical estimates of pulsar periods with observational data. Section 5 discusses the significance of our analysis, and Section 6 presents our conclusions. Appendices A and B provide details of frequency and period derivations.

2 Spindown Mechanisms

As radio pulsars age, they tend to lose rotational energy through various physical processes. The dominant mechanism for this energy loss is magnetic dipole radiation [42][43]. Gravitational wave emission, which is a quadrupole-type radiation, becomes significant for younger pulsars. This section focuses on the impact of current-type r-mode energy loss on pulsar

spin-down [44][45][46][47]. Recent studies have provided simplified expressions for damping rates by bulk and shear viscosity [48]. These expressions help refine our theoretical models of r-mode damping ([49]).

Energy losses are generally inferred from the rates of change of energy [50],

$$\dot{E}_{\text{mono}} = -\beta \frac{\mu}{cR^2} \Omega^2, \quad (2.1)$$

$$\dot{E}_{\text{dip}} = -\frac{2\mu^2}{3c^3} \Omega^4, \quad (2.2)$$

and

$$\dot{E}_{\text{quad}} = -\frac{32GI^2e^2}{5c^5} \Omega^6, \quad (2.3)$$

where $\Omega = 2\pi\nu$, ν is the pulsar rotational frequency, β is a dimensionless factor, μ is the magnetic moment perpendicular to the pulsar angular frequency vector Ω , R is the pulsar radius, I is the pulsar's moment of inertia, and e is its ellipticity. The variation in the moment of inertia affects fast-spinning pulsars with a period $P < 1.5$ ms. Although physical processes such as phase transitions in the interior of the fast-rotating neutron stars can produce changes in the moment of inertia [51], for slowly rotating pulsars with a period $P \geq 3$ ms, the variation of I can be neglected [50].

The rate of change of frequency can be related to the rate of change of energy by considering the rotational kinetic energy,

$$\begin{aligned} E_{\text{rot}} &= \frac{1}{2} I \Omega^2, \\ \implies \dot{\nu} &= \frac{1}{4\pi^2 I} \frac{\dot{E}_{\text{rot}}}{\nu}. \end{aligned} \quad (2.4)$$

Equation (2.4) captures the contributions to spin-down from different energy loss mechanisms. It is useful to express the spin-down equation

$$\dot{\nu} = k\nu^n \quad (2.5)$$

in a more general form using a Taylor series expansion and setting constraints on the spin-down rate. We develop this idea further based on models discussed in Alvarez and Carramiñana [50], which considered the monopolar and dipole terms, and Chishtie et al. [41], which accounted for the effects of gravitational wave emissions. We write the spin-down equation with the additional r-mode energy loss in the following non-linear differential equation,

$$\dot{\nu} = -s(t)\nu - r(t)\nu^3 - g(t)\nu^5 - l(t)\nu^7, \quad (2.6)$$

where s , r , g , and l are referred to as spin-down coefficients.

Equations (1), (2), and (3) capture the dominant contributions at their respective powers of rotation frequency. It is true that the monopole term might involve processes unrelated to the magnetic dipole. For the quadrupole term, contributions from a magnetic quadrupole could potentially exceed those from the mass quadrupole. We acknowledge that, in principle, the magnetic quadrupole contribution may be significant. The seventh-order term in equation (6) specifically represents the r-mode energy loss. R-modes become unstable through the emission of gravitational waves, leading to a characteristic energy loss. This term is proportional to ν^7 , corresponding to a braking index $n = 7$, which accounts for the

gravitational wave emission associated with these modes [18][52][14][40][53]. The inclusion of this term is based on detailed models of neutron star dynamics, where r-modes contribute significantly to the spin-down rate at high rotational frequencies. For a comprehensive understanding of the physical basis of this term, the reader is referred to the work of Alford and Schwenzer [40], where the properties of neutron stars emitting continuous gravitational waves are investigated, and the influence of r-modes is thoroughly discussed. The octupole moment contribution may be considered for a neutron star binary system or a neutron star that exhibits non-barotropicity [54][55], but it was not considered in this work.

Gravitational waves typically amplify these oscillations in neutron stars, leading to the Chandrasekhar-Friedman-Schutz instability [56][57]. Numerical studies have shown increasing instability of the r-modes [58][59], and Andersson et al. found that r-mode instability significantly slows down the rotation of neutron stars [60]. Many studies have modeled the expected r-mode gravitational wave frequencies as functions of pulsar observables and developed detection strategies to search for these signals efficiently [61][62][63][64].

3 Analytical Expressions considering r-modes

3.1 Rotational Frequency and r-Mode Frequency

An equation stating the relationship between the r-mode angular frequency ω and the neutron star rotational angular frequency Ω is

$$\omega = -m\Omega + \frac{2m\Omega}{l(l+1)}, \quad (3.1)$$

where l and m are spherical harmonic indices used to describe the angular dependency and the number of radial nodes of the mode eigenfunction [2][65]. We consider stellar models that exhibit local barotropicity, restricting the analysis to the fundamental perturbation where $l = m = 2$ as the $m = 2$ mode is the most unstable against gravitational wave radiation among the inertial modes and gives the most significant contribution [66][67][68]. In reality, the internal structure of neutron stars is complex, with composition gradients that create buoyancy forces characterized by the Brunt-Väisälä frequency. This affects the dynamics of oscillation modes and the coupling between different multipole moments. While the assumption of barotropicity simplifies the analysis and allows us to derive analytical insights, it is a simplification. Future work should aim to incorporate the effects of stratification and the Brunt-Väisälä frequency to provide a more accurate representation of neutron star dynamics and energy dissipation mechanisms. In this analysis, we do not consider frequencies such as the Brunt-Väisälä frequency associated with internal gravity waves. The expected r-mode angular frequency ω given by $l = m$ is

$$\omega = -\frac{(l+2)(l-1)}{l+1}\Omega, \quad (3.2)$$

and the r-mode gravitational wave frequency is

$$f = -\frac{2}{3\pi}\Omega. \quad (3.3)$$

Equation (3.3) represents only the lowest order terms in an expansion in terms of the neutron star rotational angular frequency. A higher-order approximation of r-mode frequency is

$$f = A\nu - \frac{B}{\nu_k^2}\nu^3, \quad (3.4)$$

where ν is the neutron star rotational frequency in Hz, ν_k is the Keplerian frequency $\nu_k = 506$ Hz chosen by convention [52][69] with

$$\begin{aligned} 1.39 \leq A \leq 1.57, \\ 0 \leq B \leq 0.195, \end{aligned} \quad (3.5)$$

where A is given by the general relativistic corrections for slowly rotating stars [69][63][61], and B is given by the rapid rotation correction [68]. The trinomial equation (3.4) is of the exact form solvable using the multivalued Lambert-Tsallis function [70][71].

A generalization of the Lambert W function is the Lambert-Tsallis W_q function using the generalized Tsallis q -exponential [72]

$$\exp_q z = [1 + (1 - q)z]^{\frac{1}{1-q}} \text{ for } q \neq 1. \quad (3.6)$$

Although the argument of the Lambert-Tsallis $W_q(z)$ can be complex, the argument in our case satisfies

$$W_q(z) \exp_q W_q(z) = z \text{ for } z \in \mathcal{R}. \quad (3.7)$$

The exact values of the rotational frequency in equation (3.4) are given by the Lambert-Tsallis solution of a general trinomial equation in the form specified in [70][71]:

$$\nu_1 = \left[-\frac{A}{2B} \nu_k^2 W_{\frac{1}{2}} \left\{ -\frac{2B}{A \nu_k^2} \left(\frac{f}{A} \right)^2 \right\} \right]^{1/2}, \quad (3.8)$$

and

$$\nu_2 = \left[\frac{3B}{2A \nu_k^2} W_{\frac{5}{2}} \left\{ \frac{2A \nu_k^2}{3B} \left(\frac{-f \nu_k^2}{B} \right)^{-2/3} \right\} \right]^{-1/2}. \quad (3.9)$$

For PSR J0537-6910, a fast-spinning young pulsar with rotational frequency $\nu = 62$ Hz [73], the estimated r-mode frequency falls into the LIGO frequency sensitivity band. The range of r-mode gravitational wave frequency given by equation (3.4) and A and B coefficients in equation (3.5) is 86 – 98 Hz [74][61]. The Lambert-Tsallis rotational frequency range given by equation (3.8) using the same A and B coefficients in equation (3.5) and r-mode gravitational wave frequency range is $62.00 \leq \nu_1 \leq 62.42$ Hz. Values given by equation (3.9) are too large to be physically relevant.

3.2 Compactness and r-Mode Frequency

The compactness of a neutron star is defined as $C = M/R$, mass over radius. A quadratic model for r-mode gravitational wave frequency and neutron star compactness is

$$f = a_1 \left(\frac{M}{R} \right) - a_2 \left(\frac{M}{R} \right)^2 + a_3, \quad (3.10)$$

For realistic coefficients and compactness ranges given in [62][61], small value approximation of (3.10) gives

$$f - a_3 = -a_2 \left(\frac{M}{R} \right)^2 \exp \left\{ -\frac{a_1}{a_2} \frac{R}{M} \right\}, \quad (3.11)$$

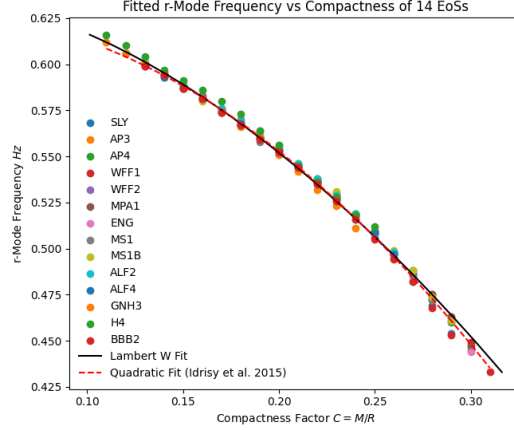


Figure 1. The r-Mode Frequency vs. Compactness results for 14 tabulated EoSs in Idrisy et al. [62]. The Lambert W r-mode gravitational wave frequency solution in equation (3.12) is compared with the quadratic model equation (3.10). The Lambert W solution coefficients are $a_1 = -0.184$, $a_2 = 1.640$, and $a_3 = 0.667$ with R^2 value 0.9972. The quadratic model coefficients are $a_1 = 0.079$, $a_2 = 2.25$, and $a_3 = 0.627$ as given in [62].

We obtain the following relationship between the compactness C of a neutron star and its r-mode gravitational wave frequency from equation (3.11),

$$C = \frac{M}{R} = \frac{a_1}{2a_2} \left(W \left\{ \frac{a_1}{2a_2} \sqrt{\frac{a_2}{a_3 - f}} \right\} \right)^{-1}, \quad (3.12)$$

where W is the Lambert W function defined by $W(z) \exp\{W(z)\} = z$ [75].

In Figure 1, we fit the analytical solution equation (3.12) to r-mode gravitational wave frequency vs. compactness values using 14 different EoS models in [62] and find the best fit is given by $a_1 = -0.184$, $a_2 = 1.640$, and $a_3 = 0.667$, with R^2 value 0.9972. Equation (3.12) gives directly fitted neutron star compactness and r-mode gravitational wave frequency expression regardless of the EoS. This enables direct substitution of neutron star compactness in further analytical derivations.

3.3 Tidal Deformability and r-Mode Frequency

Tidal interactions cause neutron stars to be distorted. In the case of a binary pulsar system, the tidal deformability parameter quantifies the tidal deformation effects due to the coalescing companion. A dimensionless tidal deformability Λ is

$$\Lambda = \frac{2}{3} k_2 \left(\frac{R}{M} \right)^5, \quad (3.13)$$

where k_2 is the $l = 2$ tidal Love number with estimated values $0.0253 < k_2 < 0.5511$ [76][77]. A quadratic model that fits the relationship between the r-mode gravitational wave frequency and the dimensionless tidal deformability quantity $\ln \Lambda$ is

$$f = b_1 \ln \Lambda + b_2 (\ln \Lambda)^2 + b_3, \quad (3.14)$$

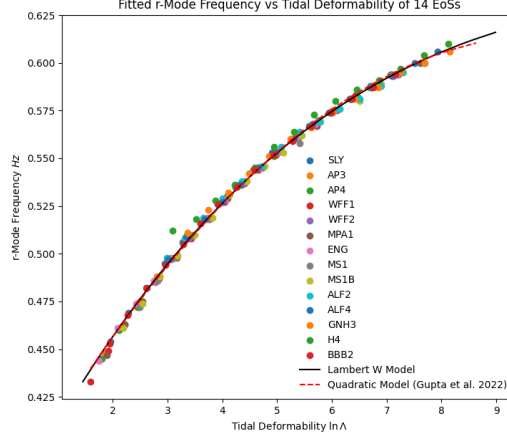


Figure 2. The r-Mode Frequency vs. Tidal Deformability results for 14 tabulated EoSs in Idrisy et al. [62] calculated using LALsuite [79]. The Lambert W model has best-fit coefficients $b_1 = 0.0568$, $b_2 = 0.0043$, and $b_3 = 0.3591$ with R^2 error 0.998. The quadratic model has best-fit coefficients $b_1 = 0.0498$, $b_2 = -0.0025$, and $b_3 = 0.3668$ in Gupta et al. [78].

where b_1 , b_2 , and b_3 are the deformability coefficients, and \ln is the natural logarithm, equivalent to \log given in Gupta et al. [78]. For realistic coefficients where $b_2/b_1 \ln \Lambda \ll 1$, an approximation of equation (3.14) is

$$-\frac{b_2}{b_1^2}(f - b_3) = -\frac{b_2}{b_1} \ln \Lambda \exp\left\{-\frac{b_2}{b_1} \ln \Lambda\right\}. \quad (3.15)$$

The Lambert W solution of the dimensionless tidal deformability quantity $\ln \Lambda$ in terms of the r-mode gravitational wave frequency is

$$\ln \Lambda = -\frac{b_1}{b_2} W\left\{-\frac{b_2}{b_1^2}(f - b_3)\right\}. \quad (3.16)$$

In Figure 2, we fit the Lambert W solution equation (3.16) to tidal deformability and r-mode gravitational wave frequency data computed using the Tolman–Oppenheimer–Volkoff equation solver in LALsuite [79] referencing the compactness data in Table 2 of Idrisy et al. [62]. The best fit is given by $b_1 = 0.0568$, $b_2 = 0.0043$, and $b_3 = 0.3591$ with R^2 error 0.998. The quadratic model equation (3.14) in Gupta et al. [78] is plotted with their best-fit coefficients $b_1 = 0.0498$, $b_2 = -0.0025$, and $b_3 = 0.3668$.

3.4 r-Mode Amplitude and Rotational Frequency

A rotating neutron star can be treated as a system with two degrees of freedom, the neutron star angular frequency Ω , and the r-mode gravitational amplitude α . We use equations detailing the evolution of these parameters from [80],

$$\frac{d\alpha}{dt} = -\frac{\alpha}{\tau_{GR}} - \frac{\alpha}{\tau_V} \frac{1 - \alpha^2 Q}{1 + \alpha^2 Q}, \quad (3.17)$$

$$\frac{d\Omega}{dt} = -\frac{2\Omega}{\tau_V} \frac{\alpha^2 Q}{1 + \alpha^2 Q}, \quad (3.18)$$

where Q is an EoS-dependent parameter defined by $Q = 3\tilde{J}/2\tilde{I}$. τ_{GR} and τ_V are the gravitational wave and viscous timescales [58]. The timescales τ_{GR} (gravitational radiation timescale) and τ_V (viscous timescale) are not constants but functions of angular frequency Ω and temperature T , as detailed in Lindblom et al. [81]. Specifically, τ_{GR} scales with Ω^{-6} and τ_V scales with Ω^n , where n depends on the viscous processes involved.

For a slowly rotating neutron star, the temperature and angular velocity change gradually, allowing these parameters to be treated as constants over short timescales. Consequently, we adopt the approach of treating the timescales as constants in our analysis, following the fiducial values provided by Owen et al. [80]. This simplifies the mathematical treatment while preserving the essential physics.

This approximation is consistent with the literature, such as Andersson et al. [82] and Ho & Lai [83], where similar assumptions are made to analyze neutron star dynamics. By clarifying the conditions under which the timescales are approximated as constants, we ensure our treatment is rigorous and well-founded. Rearranging equation (3.17) gives

$$\frac{\tau_{GR}\tau_V(1 + \alpha^2 Q)d\alpha}{\alpha[(\tau_V + \tau_{GR} + \alpha^2(\tau_V Q - \tau_{GR}Q))]} = -dt. \quad (3.19)$$

We define $\xi_1 = \tau_{GR}\tau_V$, $T_A = \tau_{GR} + \tau_V$ and $T_B = (\tau_V - \tau_{GR})Q$ and substitute the above timescale terms into equation (3.19),

$$\frac{\xi_1(1 + \alpha^2 Q)d\alpha}{\alpha(T_A + \alpha^2 T_B)} = -dt, \quad (3.20)$$

where all terms involving timescales τ_{GR} and τ_V , and the equation-of-state-dependent parameter Q are all treated as constants.

Integrating equation (3.20) and rearranging it in the Lambert W function format, we can thus express the r -mode gravitational wave amplitude α as,

$$\alpha = \left(\frac{1}{2\xi_c} W \left(2\xi_c \exp \left\{ \frac{-2(t + \xi_B \ln T_A - c_1)}{\xi_A} \right\} \right) \right)^{1/2}. \quad (3.21)$$

The neutron star rotational frequency ν relates to the angular frequency as $\nu = \Omega/(2\pi)$, we thus have an expression for the rotational frequency as a function of time. The r -mode gravitational wave amplitude α and the neutron star gravitational wave amplitude h_0 can be further related by

$$\alpha = \left(\frac{5}{8\pi} \right)^{1/2} \frac{c^5}{G} \frac{h_0}{(2\pi f)^3} \frac{d}{MR^3 J}, \quad (3.22)$$

where d is the distance to the pulsar [63].

3.5 Period and Time-Dependent Spin-down Coefficients

In this section, we perform the pulsar period analysis using the model introduced by Chishti et al. [41]. Our analysis focuses exclusively on single isolated pulsars, excluding binary systems. The spin-down coefficients $\{s, r, g, l\}$ in our model are time-dependent.

The validity of this period model was verified by comparing the braking index and frequency derivatives derived in [41] with those reported by Lyne et al. [84]. Additionally, we analyzed pulsar timing data from the ATNF Pulsar Database using our derived period equation. Our results, presented in Table 3, demonstrate that our estimated periods match the observed periods with a relative error of only 0.02%.

Our primary goal is to provide explicit relationships between various quantities involved in pulsar spin-down. These relationships are crucial for further analytical work and can serve as a foundation for future studies in the field. Transforming equation (2.6) using $P = 1/f$ and factoring out P^5 , we obtain

$$P^5 \frac{dP}{dt} = (s_0 P^6 + r_0 P^4 + g_0 P^2 + l_0) \left(1 + \frac{t}{t_c}\right)^{-2}, \quad (3.23)$$

where t_c is the characteristic timescale of field decay. Making the substitution, $K = P^2$ and $dK = 2P dP$, equation (3.23) can be written as

$$\frac{K^2 dK}{2s_0[(K-a)(K-b)(K-c)]} = \left(1 + \frac{t}{t_c}\right)^{-2} dt. \quad (3.24)$$

Integrating equation (3.24), we obtain

$$\begin{aligned} 2[(x-a)(x^2-y^2) + 2xy^2] \tan^{-1} \frac{y(K_0-K)}{(K-x)(K_0-x)+y^2} + \\ [y(x^2-y^2) - 2xy(x-a)] \ln \frac{(K-x)^2+y^2}{(K_0-x)^2+y^2} \\ - 2ya^2 \ln \frac{K-a}{K_0-a} = -4ys_0t(x^2-2ax+a^2+y^2), \end{aligned} \quad (3.25)$$

three implicit expressions for the period as a function of, which in turn depend on the spin-down coefficients. We make estimates of the period terms by considering the Crab pulsar PSR B0531+21 [85]. We numerically evaluate each of the period terms in equation (3.25) for the Crab pulsar and present the numerical values in Table 1.

Function	Value for the Crab Pulsar
$\ln \frac{(K-x)^2+y^2}{(K_0-x)^2+y^2}$	0.0158
$\tan^{-1} \frac{y(K_0-K)}{(K-x)(K_0-x)+y^2}$	-0.066
$\ln \frac{K-a}{K_0-a}$	0.0540

Table 1. Estimates for the arctan and logarithm terms in equation (3.25). The values are small enough to allow for Taylor expansions.

These values are appropriate for series expansions for the terms and we thus rewrite and simplify equation (3.25) as

$$\begin{aligned} (K-K_0) \left\{ \frac{\lambda_3}{(K-x)(K_0-x)+y^2} + \lambda_1(K+K_0-2x) + \lambda_2 \right\} = -\lambda_s t, \\ \text{where } \lambda_1 = \frac{2ax-x^2-y^2}{(q_0-x)^2+y^2}, \quad \lambda_2 = \frac{-2a^2}{K_0-a}, \\ \lambda_3 = 2(x^3-ax^2+ay^2+xy^2), \quad \lambda_s = 4s_0((x-a)^2+y^2). \end{aligned} \quad (3.26)$$

We perform simple calculations for pulsars from the Australia Telescope National Facility (ATNF) database to get numerical estimates on the values of the λ terms. We find that the term containing λ_1 tends to be much smaller than the other two on the left-hand side. We thus neglect λ_1 and continue with the analysis with λ_2 and λ_3 terms. The exact values for various pulsars can be found in Table Equation (3.26) can then be simplified as,

PSR	$\lambda_1(K + K_0 - 2x)$	λ_2	$\frac{\lambda_3}{(K-x)(K_0-x)-y^2}$	λ_s
J0007+7303	0.012	-0.60	6160.00	2.167×10^{-7}
B0531+21 (Crab)	-4.815×10^{-7}	-9.586×10^{-4}	-8.638×10^{-3}	5.589×10^{-9}
J1023-5746	0.00028	-0.52	-43.37	5.71×10^{-9}
J1418-6058	0.00025	-0.23	-650.16	1.10×10^{-8}

Table 2. Estimates of λ terms for different pulsars.

$$\begin{aligned} \alpha_1 K^2 + (\alpha_2 + \lambda_a t)K + \alpha_3 + \lambda_b t &= 0, \\ \text{where } \alpha_1 &= \lambda_2(K_0 - x), \quad \alpha_2 = \lambda_3 + \lambda_2(x^2 - y^2 - K_0^2), \\ \alpha_3 &= K_0(\lambda_2(K_0 x - x^2 + y^2) - \lambda_3), \quad \lambda_a = -\lambda_s(K_0 - x), \\ &\text{and } \lambda_b = -\lambda_s(K_0 x - x^2 + y^2). \end{aligned} \quad (3.27)$$

We find the roots of equation (3.27) using the quadratic formula and observe only one of the two roots gives values in agreement with the data. Hence the period can then be written as

$$P(t) = \sqrt{\frac{1}{2\alpha_1} \{-\alpha_2 - \lambda_a t + \sqrt{(\alpha_2 + \lambda_a t)^2 - 4\alpha_1(\alpha_3 + \lambda_b t)}\}} \quad (3.28)$$

Table 3 shows estimates of different parameters in equation (3.28). We compute the parameter values and estimate the period at different times for the Crab pulsar PSR B0531+21, which has been studied in the context of r-modes in the past [86][87].

Ensuring the term in the inner square root to be positive, the range of time t in equation (3.28) is

$$t^2 \leq \frac{(2\lambda_a \alpha_2 - 4\alpha_1 \lambda_b)^2}{4\lambda_a^2(\alpha_2^2 - 4\alpha_1 \alpha_3)} \quad (3.29)$$

Equation (3.28), which has been derived from the solution of the cubic equation, gives the analytical solution of the period $P(t)$ in terms of physical quantities such as period, spin-down coefficients, and pulsar rotational frequency. It is useful for determining the pulsar characteristic age.

3.6 Braking Indices

Equation (2.5) is the simplest formulation of pulsar spin-down which relates the rate of change of frequency to a power of the frequency itself. The power n is referred to as the braking index, where ν is the rotational frequency of the pulsar, k is a constant. For purely magnetic dipole radiation in a vacuum, this index takes a value of 3 [88]. The braking index of a pulsar is determined by the physical processes that cause the pulsar to spin down. $n = 1$

PSR	Parameter/Variable	Value
Crab PSR B0531+21	α_1	-3.967×10^{-8}
	α_2	2.284×10^{-9}
	α_3	-2.489×10^{-12}
	λ_a	1.104×10^{-20}
	λ_b	-7.376×10^{-23}
	P_0	33.333 ms
	P (calculated)	33.808 ms
	P (observed)	33.814 ms

Table 3. Values for estimated parameters in equation (3.28). The rotational periods were taken from the Jodrell Bank data from Modified Julian Date (MJD) 46812 to 60050. The relative error between the calculated and observed values of the period is 0.02% [85].

implies mass loss, pulsar wind, or particle acceleration processes; $n = 3$ arises due to a pure magnetic dipole moment; $n = 5$ corresponds to the lowest order gravitational wave emission. The braking indices in terms of the frequency derivatives are given as

$$n = \frac{\ddot{\nu}\nu}{\dot{\nu}^2}, \quad (3.30)$$

and

$$m = \frac{\ddot{\nu}\nu^2}{\dot{\nu}^3}. \quad (3.31)$$

Furthermore, [48] has highlighted the significant impact of r-mode instabilities on the braking indices of pulsars. The simplified expressions for damping rates by bulk and shear viscosity provide a more accurate theoretical framework, allowing for better predictions of braking indices in the presence of r-mode instabilities [89].

We rewrite the braking indices in terms of the spin-down coefficients in equation (2.6). Differentiating the equation and substituting the expressions for the frequency derivatives gives the following braking indices:

$$n = \frac{s + 3r\nu^2 + 5g\nu^4 + 7l\nu^6}{s + r\nu^2 + g\nu^4 + l\nu^6} \quad (3.32)$$

$$m = \frac{s + 3r\nu^2 + 5g\nu^4 + 7l\nu^6}{s + r\nu^2 + g\nu^4 + l\nu^6} + 2\nu^2 \frac{3r + 10g\nu^2 + 21l\nu^4}{s + r\nu^2 + g\nu^4 + l\nu^6} \quad (3.33)$$

Table 4 gives numerical estimates of m and n for 4 selected pulsars.

Equations (3.32) and (3.33) provide a way to represent the braking indices of a pulsar in terms of the spin-down coefficients for an analysis that takes the r-modes in a pulsar into account.

PSR	Type	n	m
B0531+21 (Crab)	Estimation	2.33	45.33
	Observation	2.32	45.33
B1509-58	Estimation	2.83	13.53
	Observation	2.84	14.5
J1023-5746	Estimation	66.71	297314.50
	Observation	66.8	298000
J1418-6058	Estimation	29.96	2436392.81
	Observation	30.02	2460000

Table 4. Numerical estimates of braking indices for 4 pulsars from the ATNF database. ‘Observation’ values were calculated directly from the frequency derivatives whereas ‘Estimation’ values were calculated using the spindown coefficients in Table 5. Large braking indices of J1023-5746 and J1418-6058 imply the presence of glitches at the times of measurement [90].

4 Period Analysis with Glitching Crab Pulsar PSR B0531+21 Data

PSR	Crab	J1023-5746	J1418-6058	B2234+61
f (Hz)	29.947	8.971	9.044	2.019
s (Hz)	1.28×10^{-10}	2.97×10^{-6}	5.37×10^{-6}	2.58×10^{-6}
r (Hz $^{-1}$)	-3.43×10^{-13}	-1.09×10^{-7}	-1.91×10^{-7}	-1.87×10^{-6}
g (Hz $^{-3}$)	3.22×10^{-16}	1.34×10^{-9}	2.27×10^{-9}	4.49×10^{-7}
l (Hz $^{-5}$)	-9.36×10^{-20}	-5.46×10^{-12}	-8.96×10^{-12}	-3.60×10^{-8}

Table 5. Spin-down parameters for four selected pulsars from the Australia Telescope National Facility Pulsar Database [91].

In this section, we validate the period model in equation (3.28) according to the Crab pulsar monthly ephemeris in CGRO (Compton Gamma-ray Observatory) format from Jodrell Bank Observatory [85]. We use Barycentric Dynamic Time (TDB) in seconds, which is the infinite-frequency geocentric UTC arrival time of a pulse. The TDB of observation ranges from 1987 January to 2023 September. We gather the Modified Julian Date (MJD) of glitches from the glitch table in the notes of monthly ephemeris from Jodrell Bank Observatory Pulsar Timing Results, which was updated in 2018 February including the last significant glitch in 2017 November. Some glitches suddenly decrease the frequency derivatives $\dot{\nu}$ followed by an exponential recovery step [92], we consider the dates of glitches as breaking points in our fitting model. The Taylor expansion of pulsar frequency is:

$$f(t) = f_0 + f'_0(t - t_0) + \frac{1}{2}f''_0(t - t_0)^2 + \frac{1}{6}f'''_0(t - t_0)^3 + \frac{1}{24}f''''_0(t - t_0)^4 + \delta f(t). \quad (4.1)$$

We calculate the observed frequency estimates and their derivatives between glitches recorded in Table 3 of Lyne et al. [92], from 1987 January (MJD 46798), as shown in Table 6. We set the mid-point of the Taylor expansion before the first glitch break point to MJD 47084. Figure 3 shows the long-term fit and fits between glitches plotted against the observational data. Glitches create inconsistency in the long-term pulsar frequency evolution when compared to fits between glitches. Fits between glitches tails closely to the observation data with an average difference $P(t) - P_{\text{obs}} = -1.166 \times 10^{-7}$. The long-term fit has a small deviation compared to the observation data with an average difference of -6.105×10^{-5} . The long-term fit from MJD 53250 to 54000 underestimates the pulsar period due to a glitch causing additional spin-down in rotational frequency as shown in Figure 3. Figure 4 shows the relative difference between the long-term fit, fits between glitches, and the observational data respectively. The long-term fit relative difference shows an exponential curve as time progresses without correcting for the glitch. For fits between glitches, sharp and sudden increases in relative difference indicate the existence of potential glitch activities from MJD 50000 to 54000 [92].

A higher order of rotational frequency derivative indicates one possible source of the spin-down. For Crab pulsar, the inclusion of the fourth derivative in frequency expansion corresponds to the r-mode. In our derived model in equation (3.28), there is a trend of underestimating the period at the beginning of the glitch. After the glitch, the period evolution converges quickly to the observation. This trend between observation and the fitted result between glitches indicates that glitches do not only influence the rotational frequency, but their effects could show up in gravitational waves emitted by the pulsar.

Glitch Range	t_0	f_0	f'_0	f''_0	f'''_0	f''''_0
- 47767.4	47084	29.99	-3.786×10^{-10}	2.367×10^{-21}	-1.23×10^{-24}	4.567×10^{-24}
47767.4 - 48945.8	48331	29.95	-3.777×10^{-10}	1.138×10^{-20}	-5.469×10^{-26}	5.353×10^{-25}
48945.8 - 50259.9	49580	29.91	-3.764×10^{-10}	1.196×10^{-20}	-6.184×10^{-25}	1.257×10^{-23}
50259.9 - 51452.3	50829	29.87	-3.752×10^{-10}	1.039×10^{-20}	-1.492×10^{-24}	-4.883×10^{-24}
51452.3 - 51739.4	51619	29.84	-3.746×10^{-10}	5.456×10^{-21}	-6.928×10^{-26}	2.247×10^{-25}
51739.4 - 51804.9	51749	29.84	-3.744×10^{-10}	-1.243×10^{-20}	-2.072×10^{-27}	-3.101×10^{-26}
51804.9 - 52083.8	51955	29.83	-3.743×10^{-10}	5.34×10^{-21}	3.477×10^{-26}	-1.286×10^{-25}
52146 - 52497.3	52291	29.82	-3.74×10^{-10}	9.829×10^{-21}	2.313×10^{-25}	-4.427×10^{-25}
52497.3 - 52587.1	52562	29.81	-3.738×10^{-10}	6.738×10^{-22}	3.871×10^{-27}	2.776×10^{-26}
52587.1 - 53067.1	52806	29.81	-3.735×10^{-10}	1.005×10^{-20}	-1.869×10^{-25}	-1.641×10^{-25}
53067.1 - 53254.2	53142	29.79	-3.735×10^{-10}	4.48×10^{-20}	-8.353×10^{-25}	-2.68×10^{-24}
53331.1 - 53790	53568	29.78	-3.731×10^{-10}	8.646×10^{-21}	1.141×10^{-25}	1.074×10^{-24}
53790 - 54580	54146	29.76	-3.724×10^{-10}	1.099×10^{-20}	2.774×10^{-26}	1.113×10^{-24}
54580 - 55785	55152	29.73	-3.714×10^{-10}	1.167×10^{-20}	-3.152×10^{-24}	3.414×10^{-24}
55785 - 57839	56794	29.68	-3.699×10^{-10}	1.158×10^{-20}	-3.351×10^{-25}	6.248×10^{-24}
57839 - 58065	57981	29.64	-3.687×10^{-10}	4.901×10^{-21}	-2.963×10^{-26}	-6.696×10^{-26}
58065 - 60202	59138	29.6	-3.68×10^{-10}	1.169×10^{-20}	-3.415×10^{-24}	1.13×10^{-23}

Table 6. Frequency and its derivatives estimated using equation (4.1). Two glitch periods, MJD 52083.8 - 52146 and MJD 53254.2 - 53331.1, were removed from the spin-down estimation due to contiguous observational data [92].

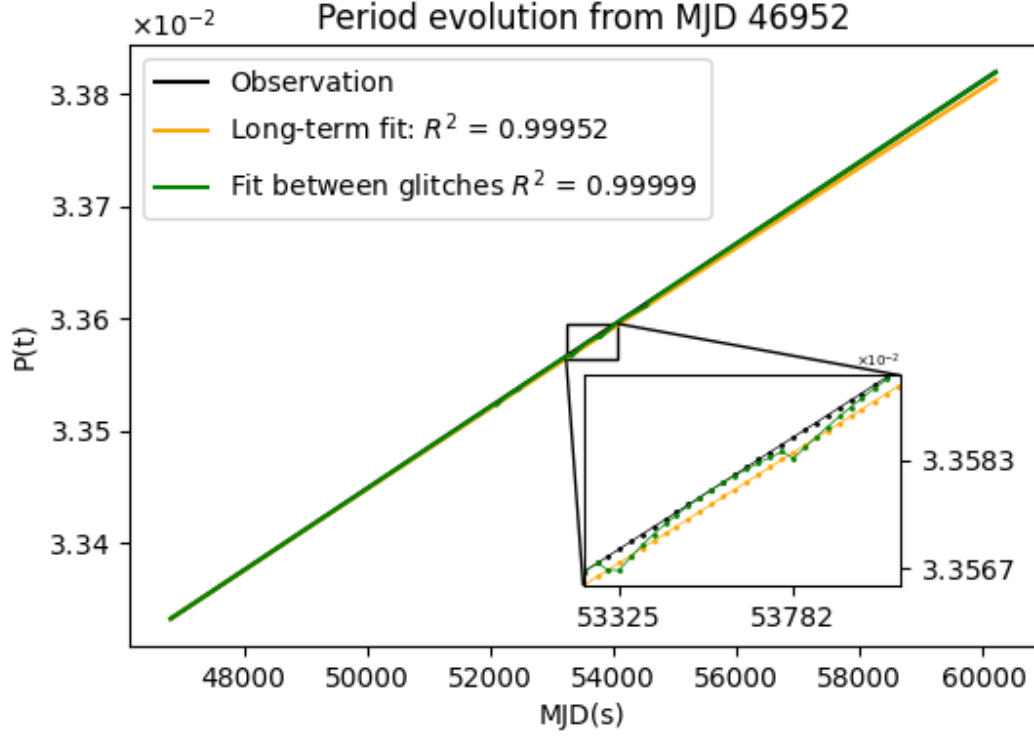


Figure 3. Period $P(t)$ evolution with respect to MJD in seconds. The zoomed-in region between MJD 52350 to 54000 shows frequency spin-down caused by glitches at MJD 53325 and MJD 53782.

5 Discussion

Continuous gravitational waves in narrow frequency bands are expected from systems such as rotating neutron stars and binary compact objects. Rotating neutron stars with irregularities or 'mountains' on their surfaces are notable examples of systems that emit these waves. Continuous gravitational waves can be used to study neutron star properties and offer further insights into their inner physics [18]. [48] have done a thorough analysis on the saturation of the r -mode instability and found it is extremely small. Although continuous gravitational waves have not been detected yet, data analysis techniques [93][94] and gravitational wave detector sensitivities [95][96][97][98][99][64] are constantly being improved. Searches for gravitational wave emissions caused by r -modes have also been carried out for specific pulsars, for example, J0537-6910 [74]. Albeit unsuccessful in detecting such sources, these attempts have reported constraints on the gravitational wave frequencies and amplitudes. If situations arise where only r -mode gravitational waves are detected, equations (3.12) and (3.16), which give the estimated neutron star compactness and tidal deformability, can infer the physics of the interior of neutron stars.

Analyzing the spin-down in pulsars and studying their braking indices offers valuable insights into both the detection of continuous gravitational waves and the analysis of pulsar timing residuals. Our time-dependent pulsar r -mode gravitational wave amplitude and pulsar rotational frequency functions provide a direct link between observable pulsar properties and the weak gravitational wave signals expected from them. This is consistent with the findings

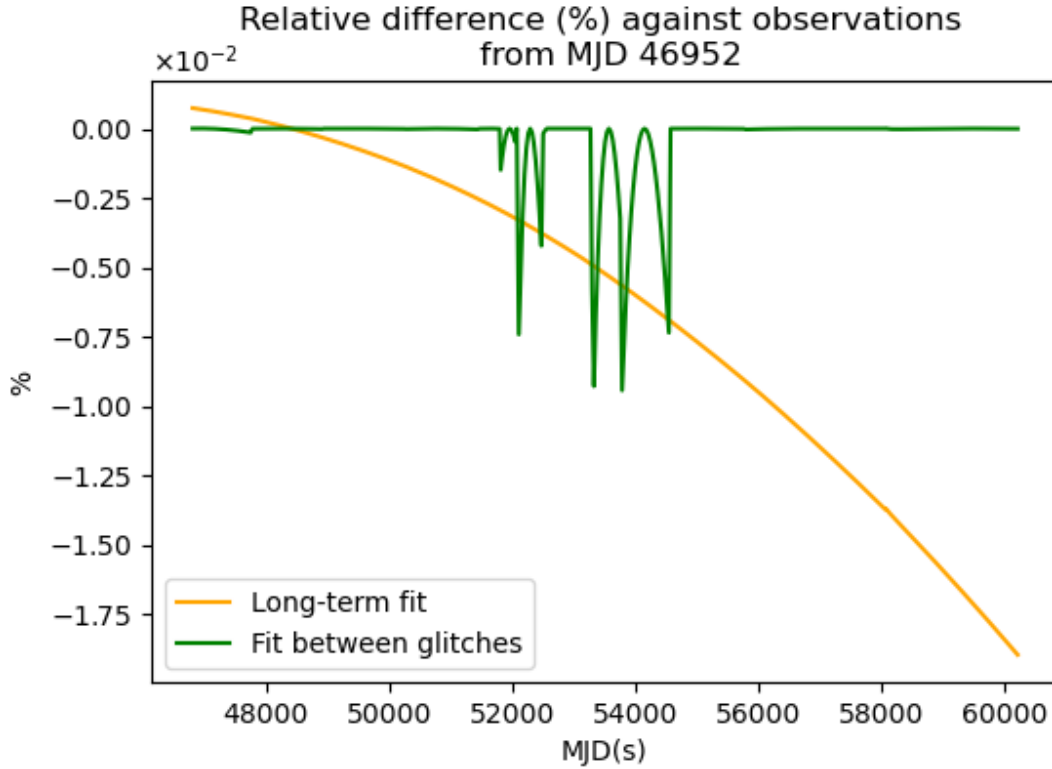


Figure 4. Relative difference between observation data and two fitting models. The long-term fit relative difference indicates an exponential increase in the period estimation error. The fit between glitches has a few sharp and sudden differences between MJD 51000 and 54580.

of Reznia [100], who demonstrated that angular momentum exchange during Type I X-ray bursts leads to significant frequency drifts. These frequency drifts are crucial for understanding the rotational dynamics of neutron stars and for refining gravitational wave detection methods, thereby contributing significantly to the field of gravitational wave astronomy. In addition, we also provide relations connecting r-mode gravitational wave frequency with neutron star gravitational wave frequency and amplitude. By integrating these relationships, we obtain direct and time-dependent estimations of pulsar gravitational wave signals and their physical properties.

The fitted compactness, tidal deformability, and r-mode gravitational wave frequency models give direct and analytical EoS-independent relationships that can be substituted into our time-dependent pulsar period models for further analysis. Our work applies to pulsars in their non-linear saturation phases where the r-modes contribute to the frequency spin-down with a seventh-order frequency term [58]. Among the four terms we consider in the spin-down equation, we find that the highest pulsar energy loss generally comes from the magnetic dipole radiation term whereas the lowest comes from the r-modes. However, modeling the spin-down behavior due to r-modes will lead to more precise pulsar timing array frequency estimations and accurate data analysis of continuous gravitational waves. Pulsar spin-down coefficients decrease for higher frequency derivatives and become increasingly difficult to measure. Our analysis allows for negative spin-down coefficients to account for glitches and spin-ups.

Numerical results comparing the long-term fit and fits between glitches indicate that Crab pulsar glitches produced cumulative exponential decreases in the rotational frequency. A theoretical model of the glitch behavior as a function of a pulsar’s frequency and period evolution is desirable instead of rough exponential decay models [92]. We will extend the analysis using our period model to other known pulsars, for example, the Big Glitch PSR J0537-6910, which has elaborate ephemeris and recording of glitches [101]. A higher order of the frequency derivatives might be over-fitting. But it is worthwhile to have a test over that the overestimated magnitude of the glitch predicts the time of the next glitch with higher accuracy. Our theoretical model with r-modes could contribute to F/G statistics and 5n-vector models which are used in the detection of gravitational waves from pulsars [74]. Our expressions of pulsar frequency terms and their derivatives as functions of time can help model pulsar timing residuals by accounting for spin changes or glitches in the timing analysis. The higher frequency terms embedded in our model give a simple framework with higher accuracy. The one-to-one mapping between the rotational period derivative and parameters of the high order can help simulate a more accurate phase evolution. This model should be applied to the detection of GW from pulsars [11], after tests on pulsars with more accurate phase evolution are performed.

6 Conclusions

In this work, we discussed pulsar spin-down mechanisms and considered the impact of r-modes in pulsar spin-down. We solved the non-linear differential equation incorporating the contribution of the r-modes to obtain time-dependent rotational frequency and period functions. Our numerical analysis is in accord with observations for the Crab pulsar. We also presented and numerically verified the braking indices in terms of spin-down coefficients with the inclusion of r-modes.

The Lambert W solutions of neutron star compactness and tidal deformability provide analytical relationships between these physical properties and the r-mode gravitational wave frequency, independent of the neutron star’s equation of state (EoS). By employing analytical solutions with known special functions such as the Lambert-Tsallis and the Lambert W function, we gain direct insights into the mathematical relationships between these quantities. This approach is instrumental in constraining the parameter space for r-mode gravitational wave frequency searches. The inclusion of r-modes significantly enhances our ability to measure the neutron star EoS [102].

Gravitational waves emitted by young pulsars might be detected as strong sources from single spindown events or as a stochastic background made up of many weaker sources [80]. With the advent of 3rd generation gravitational wave detectors and rapid improvements in detector technology, incorporating r-modes in spindown analysis offers a promising opportunity to disentangle individual events from the stochastic gravitational wave background. This advancement not only facilitates the detection of continuous gravitational waves but also enhances our understanding of neutron star interiors and their dynamic processes. We share the optimism of Arras et. al. [48] that the *r*-mode signal from both newly-born neutron star and low-mass x-ray binaries (LMXB) in the spindown phase of Levins limit cycle will be detectable by enhanced LIGO detectors. Furthermore, as demonstrated in [103], measuring this shift could be instrumental in enhancing the precision of gravitational wave detection, thereby providing significant contributions to gravitational wave astronomy.

Overall, our theoretical framework and numerical models provide a comprehensive understanding of pulsar spin-down mechanisms, incorporating r-modes' contributions. This work lays the foundation for future studies on neutron star properties and continuous gravitational wave detection, paving the way for significant advancements in astrophysics and gravitational wave astronomy.

Acknowledgements

We thank R. V. Ramos and K. Z. Nobrega at Universidade Federal do Ceará for the numerical evaluation of our Lambert-Tsallis solutions and valuable discussions. We thank Dr. Reed Essick (CITA) for valuable and informative discussions. We are grateful to the Mathematics of Information Technology and Complex Systems (MITACS) Globalink program for providing the platform and funding for this project.

A Frequency Cubic Roots with Time-independent Coefficients

For constant spin-down coefficients, equation (2.6) can be rewritten as

$$-dt = \frac{1}{\nu} \frac{d\nu}{s + r\nu^2 + g\nu^4 + l\nu^6}, \quad (\text{A.1})$$

where we use a fourth spin-down coefficient l for the f^7 term.^c We then make the substitution $\nu^2 = x$ then $d\nu = dx/2\sqrt{x}$. This allows us to write the polynomial in the denominator as a cubic that can then be factorized:

$$\frac{1}{2lx} \frac{dx}{(x-a)(x-b)(x-c)} = -dt, \quad (\text{A.2})$$

where $\{a, b, c\}$ are the roots of the cubic polynomial which can be expressed analytically or computed numerically.

The cubic roots $\{a, b, c\}$ can be analytically expressed using the general cubic formula:

$$\begin{aligned} \{x_i\} &= -\frac{1}{3} \left(\frac{r}{s} + \epsilon^i C + \frac{\Delta_0}{\epsilon^i C} \right), \\ \text{where } \epsilon &= \frac{-1 + i\sqrt{3}}{2}, \\ C &= \sqrt[3]{\frac{\Delta_1 \pm \sqrt{\Delta_1^2 - 4\Delta_0^3}}{2}}, \\ \Delta_0 &= \frac{g^2}{l} - 3\frac{r}{l}, \\ \text{and } \Delta_1 &= 2\frac{g^3}{l} - 9\frac{gr}{l^2} + 27\frac{s}{l}. \end{aligned} \quad (\text{A.3})$$

We substitute the values $\{0, 1, 2\}$ for i to get exact expressions for a, b and c , and the above can be written in a compact form using the complex cube root:

$$\begin{aligned} \{a, b, c\} = & \left\{ \left(\frac{-g^3}{27l^3} + \frac{gr}{6l^2} - \frac{s}{2l} \right) + \right. \\ & \left. \sqrt[3]{\left(\frac{-g^3}{27l^3} + \frac{gr}{6l^2} - \frac{s}{2l} \right)^2 + \left(\frac{r}{3l} - \frac{g^2}{9l^2} \right)^2} \right\}^{1/3} + \\ & \left\{ \left(\frac{-g^3}{27l^3} + \frac{gr}{6l^2} - \frac{s}{2l} \right) - \right. \\ & \left. \sqrt[3]{\left(\frac{-g^3}{27l^3} + \frac{gr}{6l^2} - \frac{s}{2l} \right)^2 + \left(\frac{r}{3l} - \frac{g^2}{9l^2} \right)^2} \right\}^{1/3} - \\ & \frac{g}{3l} \end{aligned} \quad (\text{A.4})$$

B Period Analysis with Cubic Roots

Following Appendix A, $\{a, b, c\}$ are the roots of the cubic in the denominator. Equation (3.24) can be simplified using partial fractions and integrating on both sides after simplification. Let P_0 and t_0 be the period and time initial conditions respectively. Substituting the initial conditions into the expression gives

$$\begin{aligned} (b-a)c^2 \ln \frac{K-c}{K_0-c} + (a-c)b^2 \ln \frac{K-b}{K_0-b} + \\ (c-b)a^2 \ln \frac{K-a}{K_0-a} = -2s_0t(b-a)(a-c)(c-b), \end{aligned} \quad (\text{B.1})$$

where $K_0 = P_0^2$ and the limits $t_c \gg t, t_0$ are applied as done in Chishtie et al [41]. In most cases, there are two complex roots and one real root with the complex roots being conjugates of each other. We write (b, c) as: $b = x + iy$, $c = x - iy$. Equation (B.1) can be rewritten as

$$\begin{aligned} & [(x-a)(x^2-y^2) + 2xy^2] \\ & \left(\ln \frac{K-c}{K_0-c} - \ln \frac{K-b}{K_0-b} \right) \\ & - 2iya^2 \ln \frac{K-a}{K_0-a} + i[y(x^2-y^2) - \\ & (x-a)2xy] \left(\ln \frac{K-c}{K_0-c} + \ln \frac{K-b}{K_0-b} \right) \\ & = -4iys_0t(x^2 - 2ax + a^2 + y^2). \end{aligned} \quad (\text{B.2})$$

The log terms are simplified using basic properties of complex logarithms to obtain the solution of (B.2) given in equation (3.25).

References

- [1] J. Papaloizou and J. E. Pringle. Gravitational radiation and the stability of rotating stars. *Monthly Notices of the Royal Astronomical Society*, 184:501–508, August 1978.
- [2] J. Provost, G. Berthomieu, and A. Rocca. Low Frequency Oscillations of a Slowly Rotating Star - Quasi Toroidal Modes. *aap*, 94:126, January 1981.

- [3] Nils Andersson and Kostas D. Kokkotas. Towards gravitational wave asteroseismology. *Monthly Notices of the Royal Astronomical Society*, 299(4):1059–1068, October 1998.
- [4] John L. Friedman and Sharon M. Morsink. Axial Instability of Rotating Relativistic Stars. *The Astrophysical Journal*, 502(2):714–720, August 1998.
- [5] S. Abbassi, M. Reutord, and V. Rezanian. An r-mode in a magnetic rotating spherical layer: application to neutron stars. *Monthly Notices of the Royal Astronomical Society*, 419(4):2893–2899, 2012.
- [6] Nils Andersson. R-Modes in Relativistic Stars. Presented at the KITP Miniprogram: R-Modes in Neutron Stars, Aug 3, 2000, Kavli Institute for Theoretical Physics, University of California, Santa Barbara, id.1, August 2000.
- [7] D. R. Lorimer and M. Kramer. *Handbook of Pulsar Astronomy*, volume 4. 2004.
- [8] J. H. Taylor and D. R. Stinebring. Recent progress in the understanding of pulsars. *araa*, 24:285–327, January 1986.
- [9] B. P. Abbott, R. Abbott, T. D. Abbott, M. R. Abernathy, K. Ackley, C. Adams, P. Addesso, R. X. Adhikari, V. B. Adya, C. Affeldt, et al. Gw150914: The advanced ligo detectors in the era of first discoveries. *Physical Review Letters*, 116:241103, 2016.
- [10] T. Akutsu, M. Ando, et al. Kagra: 2.5 generation interferometric gravitational wave detector. *Nature Astronomy*, 3(1):35–40, January 2019.
- [11] R. Abbott, T. D. Abbott, F. Acernese, et al. First search for nontensorial gravitational waves from known pulsars. *Phys. Rev. Lett.*, 120:031104, Jan 2018.
- [12] Benjamin J. Owen, Lee Lindblom, Curt Cutler, Bernard F. Schutz, Alberto Vecchio, and Nils Andersson. Gravitational waves from hot young rapidly rotating neutron stars. *Physical Review D*, 58(8):084020, October 1998.
- [13] Lars Bildsten and Greg Ushomirsky. Viscous Boundary-Layer Damping of R-Modes in Neutron Stars. *The Astrophysical Journal Letters*, 529(1):L33–L36, January 2000.
- [14] N. Andersson, D. I. Jones, and K. D. Kokkotas. Strange stars as persistent sources of gravitational waves. *Monthly Notices of the Royal Astronomical Society*, 337(4):1224–1232, December 2002.
- [15] Brynmor Haskell, Nathalie Degenaar, and Wynn C. G. Ho. Constraining the physics of the r-mode instability in neutron stars with X-ray and ultraviolet observations. *Monthly Notices of the Royal Astronomical Society*, 424(1):93–103, July 2012.
- [16] Vahid Rezanian. r-Modes in the Ocean of a Magnetic Neutron Star. *The Astrophysical Journal*, 574(2):899–907, August 2002.
- [17] F. A. Chishtie, Xiyang Zhang, and S. R. Valluri. An analytic approach for the study of pulsar spindown. *Classical and Quantum Gravity*, 35(14):145012, July 2018.
- [18] Neil Lu, Karl Wette, Susan M. Scott, and Andrew Melatos. Inferring neutron star properties with continuous gravitational waves. *mnras*, 521(2):2103–2113, May 2023.
- [19] Firstname1 Author1, Firstname2 Author2, and Firstname3 Author3. The title of the paper. *The Astrophysical Journal*, 923(1):14, 2021.
- [20] J. Aasi, B. P. Abbott, R. Abbott, T. Abbott, M. R. Abernathy, K. Ackley, C. Adams, T. Adams, P. Addesso, R. X. Adhikari, and et al. Advanced ligo. *Classical and Quantum Gravity*, 32(7):074001, 2015.
- [21] F. Acernese, M. Agathos, K. Agatsuma, D. Aisa, N. Allemandou, A. Allocca, J. Amarni, P. Astone, G. Balestri, G. Ballardin, and et al. Advanced virgo: a second-generation interferometric gravitational wave detector. *Classical and Quantum Gravity*, 32(2):024001, 2015.

- [22] T. Akutsu, M. Ando, K. Arai, Y. Arai, S. Araki, H. Araya, N. Arima, A. Araya, K. Aso, Y. Aso, and et al. Overview of kagra: Detector design and construction history. *Progress of Theoretical and Experimental Physics*, 2019(5):05A101, 2019.
- [23] Marica Branchesi, Michele Maggiore, David Alonso, Charles Badger, et al. Science with the einstein telescope: a comparison of different designs, 2023.
- [24] Matthew Evans, Rana X Adhikari, Chaitanya Afle, et al. A horizon study for cosmic explorer: Science, observatories, and community, 2021.
- [25] Pau Amaro-Seoane, Heather Audley, Stanislav Babak, John Baker, et al. Laser interferometer space antenna, 2017.
- [26] W.-H. Ruan, Z.-K. Guo, R.-G. Cai, and Y.-Z. Zhang. Taiji program: Gravitational-wave sources. *International Journal of Modern Physics A*, 35(17):2050075, 2020.
- [27] J. Luo, L.-S. Chen, H.-Z. Duan, Y.-G. Gong, S. Hu, J. Ji, Q. Liu, J. Mei, V. Milyukov, M. Sazhin, Y.-Y. Shao, Z.-G. Silan, Z.-K. Hu, M.-E. Tobar, Y. Wang, H. Wang, Y. Xu, M. Yan, Y.-L. Zhang, and Z.-B. Zhou. Tianqin: a space-borne gravitational wave detector. *Classical and Quantum Gravity*, 33(3):035010, 2016.
- [28] Jr. Taylor, Joseph H. Millisecond pulsars: nature’s most stable clocks. *IEEE Proceedings*, 79:1054–1062, July 1991.
- [29] D. N. Matsakis, J. H. Taylor, and T. Marshall Eubanks. A statistic for describing pulsar and clock stabilities. *aap*, 326:924–928, October 1997.
- [30] R N Manchester. The international pulsar timing array. *Classical and Quantum Gravity*, 30(22):224010, nov 2013.
- [31] G Hobbs, A Archibald, Z Arzoumanian, D Backer, et al. The international pulsar timing array project: using pulsars as a gravitational wave detector. *Classical and Quantum Gravity*, 27(8):084013, apr 2010.
- [32] Hamsa Padmanabhan and Abraham Loeb. Unravelling the formation of the first supermassive black holes with the ska pulsar timing array, 2023.
- [33] J. Antoniadis, P. Arumugam, S. Arumugam, et al. The second data release from the european pulsar timing array iii. search for gravitational wave signals, 2023.
- [34] Pratik Tarafdar, K Nobleson, et al. The indian pulsar timing array: First data release. *Publications of the Astronomical Society of Australia*, 39, 2022.
- [35] Andrew Zic, Daniel J. Reardon, Agastya Kapur, George Hobbs, Rami Mandow, Małgorzata Curyło, Ryan M. Shannon, Jacob Askew, Matthew Bailes, N. D. Ramesh Bhat, Andrew Cameron, Zu-Cheng Chen, Shi Dai, Valentina Di Marco, Yi Feng, Matthew Kerr, Atharva Kulkarni, Marcus E. Lower, Rui Luo, Richard N. Manchester, Matthew T. Miles, Rowina S. Nathan, Stefan Osłowski, Axl F. Rogers, Christopher J. Russell, Renée Spiewak, Nithyanandan Thyagarajan, Lawrence Toomey, Shuangqiang Wang, Lei Zhang, Songbo Zhang, and Xing-Jiang Zhu. The parkes pulsar timing array third data release, 2023.
- [36] Heng Xu, Siyuan Chen, et al. Searching for the nano-hertz stochastic gravitational wave background with the chinese pulsar timing array data release i. *Research in Astronomy and Astrophysics*, 23(7):075024, June 2023.
- [37] Gabriella Agazie, Akash Anumalapudi, Anne M. Archibald, others, and Nanograv Collaboration. The NANOGrav 15 yr Data Set: Evidence for a Gravitational-wave Background. *apjl*, 951(1):L8, July 2023.
- [38] A. Weltman, P. Bull, S. Camera, K. Kelley, et al. Fundamental physics with the square kilometre array. *Publications of the Astronomical Society of Australia*, 37, 2020.

- [39] W. C. G. Ho, N. Andersson, and B. Haskell. Revisiting the r-mode instability window of accreting neutron stars. *Physical Review Letters*, 107(10):101101, 2011.
- [40] Mark G. Alford and Kai Schwenzer. The instability and non-linear dynamics of rotating stars. *Monthly Notices of the Royal Astronomical Society*, 437(2):1220–1235, 2014.
- [41] F A Chishtie, Xiyang Zhang, and S R Valluri. An analytic approach for the study of pulsar spindown. *Classical and Quantum Gravity*, 35(14):145012, jun 2018.
- [42] T. Gold. Rotating Neutron Stars as the Origin of the Pulsating Radio Sources. *Nature*, 218(5143):731–732, May 1968.
- [43] F. Pacini. Rotating Neutron Stars, Pulsars and Supernova Remnants. *Nature*, 219(5150):145–146, July 1968.
- [44] J. P. Ostriker and J. E. Gunn. On the Nature of Pulsars. I. Theory. *The Astrophysical Journal*, 157:1395, September 1969.
- [45] Attilio Ferrari and Remo Ruffini. Theoretical Implications of the Second Time Derivative of the Period of the Pulsar NP 0532. *apjl*, 158:L71, November 1969.
- [46] J. Papaloizou and J. E. Pringle. Non-radial oscillations of rotating stars and their relevance to the short-period oscillations of cataclysmic variables. *Monthly Notices of the Royal Astronomical Society*, 182(3):423–442, 03 1978.
- [47] Nils Andersson. A new class of unstable modes of rotating relativistic stars. *The Astrophysical Journal*, 502(2):708–713, aug 1998.
- [48] Phil Arras, Eanna E. Flanagan, Sharon M. Morsink, A. Katrin Schenk, Saul A. Teukolsky, and Ira Wasserman. Saturation of the r-Mode Instability. *The Astrophysical Journal*, 591(2):1129–1151, July 2003.
- [49] L. Lindblom, J. E. Tohline, and M. Vallisneri. Nonlinear evolution of the r-modes in neutron stars. *Astrophysical Journal*, 591:1129–1151, 2003.
- [50] Alvarez, C. and Carramiñana, A. Monopolar pulsar spin-down. *A&A*, 414(2):651–658, 2004.
- [51] Norman K. Glendenning, S. Pei, and F. Weber. Signal of quark deconfinement in the timing structure of pulsar spin-down. *Phys. Rev. Lett.*, 79:1603–1606, Sep 1997.
- [52] Yuri Levin and Greg Ushomirsky. Crust-core coupling and r-mode damping in neutron stars: a toy model. *mnras*, 324(4):917–922, July 2001.
- [53] Kip S. Thorne. Multipole expansions of gravitational radiation. *Rev. Mod. Phys.*, 52:299–339, Apr 1980.
- [54] Paolo Pani, Leonardo Gualtieri, and Valeria Ferrari. Tidal love numbers of a slowly spinning neutron star. *Phys. Rev. D*, 92:124003, Dec 2015.
- [55] A. Mastrano, P. D. Lasky, and A. Melatos. Neutron star deformation due to multipolar magnetic fields. *Monthly Notices of the Royal Astronomical Society*, 434(2):1658–1667, 2013.
- [56] S. Chandrasekhar. Solutions of Two Problems in the Theory of Gravitational Radiation. *Physical Review Letters*, 24(11):611–615, March 1970.
- [57] J. L. Friedman and B. F. Schutz. Lagrangian perturbation theory of nonrelativistic fluids. *The Astrophysical Journal*, 221:937–957, May 1978.
- [58] Lee Lindblom, Benjamin J. Owen, and Sharon M. Morsink. Gravitational radiation instability in hot young neutron stars. *Physical Review Letters*, 80(22):4843–4846, jun 1998.
- [59] Lee Lindblom, Joel E. Tohline, and Michele Vallisneri. Nonlinear evolution of the r-modes in neutron stars. *Physical Review Letters*, 86(7):1152–1155, feb 2001.

- [60] Nils Andersson, Kostas D. Kokkotas, and Nikolaos Stergioulas. On the relevance of the r-mode instability for accreting neutron stars and white dwarfs. *The Astrophysical Journal*, 516(1):307–314, may 1999.
- [61] Suprovo Ghosh, Dhruv Pathak, and Debarati Chatterjee. Relativistic correction to the r-mode frequency in light of multimessenger constraints. *The Astrophysical Journal*, 944(1):53, feb 2023.
- [62] Ashikuzzaman Idrisy, Benjamin J. Owen, and David I. Jones. R -mode frequencies of slowly rotating relativistic neutron stars with realistic equations of state. *Physical Review D*, 91(2), jan 2015.
- [63] R. Abbott, T.D. Abbott, S. Abraham, et al. Constraints from LIGO o3 data on gravitational-wave emission due to r-modes in the glitching pulsar PSR j0537–6910. *The Astrophysical Journal*, 922(1):71, nov 2021.
- [64] R. Abbott, T.D. Abbott, S. Abraham, et al. All-sky search for continuous gravitational waves from isolated neutron stars in the early o3 LIGO data. *Physical Review D*, 104(8), oct 2021.
- [65] Nils Andersson. Gravitational waves from instabilities in relativistic stars. *Classical and Quantum Gravity*, 20(7):R105–R144, mar 2003.
- [66] Keith H. Lockitch and John L. Friedman. Where are the r-modes of isentropic stars? *The Astrophysical Journal*, 521(2):764–788, aug 1999.
- [67] Shijun Yoshida and Umin Lee. Rotational modes of nonisentropic stars and the gravitational radiation-driven instability. *The Astrophysical Journal Supplement Series*, 129(1):353–366, jul 2000.
- [68] Shijun Yoshida, Shin’ichirou Yoshida, and Yoshiharu Eriguchi. R-mode oscillations of rapidly rotating barotropic stars in general relativity: analysis by the relativistic Cowling approximation. *Monthly Notices of the Royal Astronomical Society*, 356(1):217–224, 01 2005.
- [69] Santiago Caride, Ra Inta, Benjamin J. Owen, and Binod Rajbhandari. How to search for gravitational waves from r-modes of known pulsars. *Phys. Rev. D*, 100:064013, Sep 2019.
- [70] G.B. da Silva and R.V. Ramos. The lambert–tsallis wq function. *Physica A: Statistical Mechanics and its Applications*, 525:164–170, 2019.
- [71] R. V. Ramos. Solving the fermat and fibonacci equations with the lambert-tsallis wq function, 2023.
- [72] Constantino Tsallis. Possible generalization of boltzmann-gibbs statistics. *Journal of Statistical Physics*, 52:479–487, jul 1988.
- [73] F. E. Marshall, E. V. Gotthelf, W. Zhang, J. Middleditch, and Q. D. Wang. Discovery of an Ultrafast X-Ray Pulsar in the Supernova Remnant N157B. *apjl*, 499(2):L179–L182, June 1998.
- [74] R. Abbott, T. D. Abbott, S. Abraham, F. Acernese, and LIGO Scientific Collaboration. Constraints from LIGO o3 data on gravitational-wave emission due to r-modes in the glitching pulsar PSR j0537–6910. *The Astrophysical Journal*, 922(1):71, nov 2021.
- [75] Robert Corless, Gaston Gonnet, D. Hare, David Jeffrey, and D. Knuth. On the lambert w function. *Advances in Computational Mathematics*, 5:329–359, 01 1996.
- [76] Éanna É. Flanagan and Tanja Hinderer. Constraining neutron-star tidal love numbers with gravitational-wave detectors. *Physical Review D*, 77(2), jan 2008.
- [77] Tanja Hinderer. Tidal love numbers of neutron stars. *The Astrophysical Journal*, 677(2):1216–1220, apr 2008.
- [78] Pawan Kumar Gupta, Anna Puecher, Peter T. H. Pang, Justin Janquart, Gideon Koekoek, and Chris Van Den Broeck. Determining the equation of state of neutron stars with einstein telescope using tidal effects and r-mode excitations from a population of binary inspirals, 2022.

- [79] LIGO Scientific Collaboration. LALSuite: LIGO Scientific Collaboration Algorithm Library Suite. Astrophysics Source Code Library, record ascl:2012.021, December 2020.
- [80] B. J. Owen, L. Lindblom, C. Cutler, B. F. Schutz, A. Vecchio, and N. Andersson. Gravitational waves from hot young rapidly rotating neutron stars. *Phys. Rev. D*, 58:084020, 1998.
- [81] Lee Lindblom, Benjamin J. Owen, and Sharon M. Morsink. Gravitational radiation instability in hot young neutron stars. *Physical Review Letters*, 80:4843–4846, Jun 1998.
- [82] Nils Andersson. Gravitational waves from instabilities in relativistic stars. *The Astrophysical Journal*, 502(2):708–713, 1999.
- [83] Wynn C.G. Ho and Dong Lai. Resonant excitations of rossby modes in neutron stars. *The Astrophysical Journal*, 543(1):386–400, 2000.
- [84] A. G. Lyne, R. S. Pritchard, and F. G. Smith. Crab Pulsar timing 1982–87. *Monthly Notices of the Royal Astronomical Society*, 233(3):667–676, 08 1988.
- [85] A. G. Lyne, R. S. Pritchard, and F. Graham Smith. 23 years of Crab pulsar rotational history. *mnras*, 265:1003–1012, December 1993.
- [86] Binod Rajbhandari, Benjamin J. Owen, Santiago Caride, and Ra Inta. First searches for gravitational waves from r -modes of the crab pulsar. *Phys. Rev. D*, 104:122008, Dec 2021.
- [87] Vahid Rezanian and M. Jahan-Miri. The possible role of r -modes in post-glitch relaxation of the Crab pulsar. *mnras*, 315(2):263–268, June 2000.
- [88] R. N. Manchester, J. M. Durdin, and L. M. Newton. A second measurement of a pulsar braking index. *Nature*, 313(6001):374–376, 1985.
- [89] R. Bondarescu, S. A. Teukolsky, and I. Wasserman. Spinning down newborn neutron stars: Nonlinear development of the r -mode instability. *Physical Review D*, 76:064019, 2007.
- [90] Cristóbal M. Espinoza. Braking indices and spin evolution: something is loose inside neutron stars. *Proceedings of the International Astronomical Union*, 13(S337):221–224, sep 2017.
- [91] R. N. Manchester, G. B. Hobbs, A. Teoh, and M. Hobbs. The australia telescope national facility pulsar catalogue. *The Astronomical Journal*, 129(4):1993–2006, apr 2005.
- [92] A. G. Lyne, C. A. Jordan, F. Graham-Smith, C. M. Espinoza, B. W. Stappers, and P. Weltevred. 45 years of rotation of the Crab pulsar. *Monthly Notices of the Royal Astronomical Society*, 446(1):857–864, 11 2014.
- [93] Rodrigo Tenorio, David Keitel, and Alicia M. Sintes. Search methods for continuous gravitational-wave signals from unknown sources in the advanced-detector era. *Universe*, 7(12):474, Dec 2021.
- [94] Piotr Jaranowski, Andrzej Królak, and Bernard F. Schutz. Data analysis of gravitational-wave signals from spinning neutron stars: The signal and its detection. *Phys. Rev. D*, 58:063001, Aug 1998.
- [95] B. P. Abbott, R. Abbott, T. D. Abbott, et al. Gw170817: Observation of gravitational waves from a binary neutron star inspiral. *Phys. Rev. Lett.*, 119:161101, Oct 2017.
- [96] M. Pitkin, C. Gill, D. I. Jones, G. Woan, and G. S. Davies. First results and future prospects for dual-harmonic searches for gravitational waves from spinning neutron stars. *Monthly Notices of the Royal Astronomical Society*, 453(4):4399–4420, 09 2015.
- [97] R. Abbott, H. Abe, F. Acernese, K. Ackley, N. Adhikari, and R. All-sky search for continuous gravitational waves from isolated neutron stars using advanced LIGO and advanced virgo o3 data. *Physical Review D*, 106(10), nov 2022.
- [98] R. Abbott, T. D. Abbott, F. Acernese, et al. Search for continuous gravitational waves from 20 accreting millisecond x-ray pulsars in o3 LIGO data. *Physical Review D*, 105(2), jan 2022.

- [99] R. Abbott, T. D. Abbott, F. Acernese, et al. Search of the early o3 LIGO data for continuous gravitational waves from the cassiopeia a and vela jr. supernova remnants. *Physical Review D*, 105(8), apr 2022.
- [100] Vahid Rezaia. Large frequency drifts during type i x-ray bursts. *arXiv preprint astro-ph/0304153v2*, 2003.
- [101] Wynn C G Ho, Cristóbal M Espinoza, et al. Return of the big glitcher: Nicer timing and glitches of psr j0537-6910. *Monthly Notices of the Royal Astronomical Society*, 498(4):4605–4614, 09 2020.
- [102] J.A. Faber and F.A. Rasio. Binary neutron star mergers. *Living Rev. Relativ.*, 15(8(2012)), 2012.
- [103] Yan Wang, Soumya D Mohanty, and Fredrick A Jenet. A coherent method for the detection and estimation of continuous gravitational wave signals using a pulsar timing array. *arXiv preprint arXiv:1406.5496*, 2014.